Available online at www.sciencedirect.com

ScienceDirect

journal homepage: www.elsevier.com/locate/issn/15375110

Research Paper

New concept for measuring swimming speed of free-ranging fish using acoustic telemetry and Doppler analysis

Waseem Hassan [a,*], Martin Føre [a], Henning A. Urke [b], John B. Ulvund [c], Eskil Bendiksen [d], Jo A. Alfredsen [a]

[a] Department of Engineering Cybernetics-NTNU, Trondheim, NO-7491, Norway
[b] INAQ AS, Trondheim, NO-7010, Norway
[c] Nord University, Bodø, NO-8026, Norway
[d] Bjørøya AS, Flatanger, NO-7770, Norway

ARTICLE INFO

Article history:
Received 19 October 2021
Received in revised form
14 May 2022
Accepted 17 May 2022

Keywords:
Acoustic telemetry
Doppler analysis
Marine aquaculture
Signal processing
Fish tagging

A novel technique for measuring individual fish swimming speed based on conventional acoustic telemetry and Doppler analysis was tested with live tagged fish in a field experiment at a fish farm. The aim of the experiment was to evaluate the feasibility of using this method to measure instantaneous swimming speeds over time for individual fish under commercial farming conditions. Measurements were obtained from two acoustically tagged specimen of farmed Atlantic salmon and results showed realistic speed spectra and average swimming speeds (880 mm s^{-1} std. 590 mm s^{-1} and 1080 mm s^{-1} std. 560 mm s^{-1}, corresponding to 1.4 and 1.6 body lengths per second, respectively). A reference tag moored in a stationary position in the same sea cage was simultaneously measured as having a mean speed of 110 mm s^{-1} (std. 80 mm s^{-1}), confirming that the method was able to distinguish between moving and stationary tags. Moreover, the mean speed of the reference tag was 10% of the overall speed range, agreeing with the error ranges observed for the concept in previously reported model experiments, further corroborating that the Doppler measurements were genuinely linked with tag movement. Commercially available acoustic tags with only a simple modification were used to generate the signal for the Doppler speed computation algorithm, implying that the technique will conveniently integrate with existing acoustic fish telemetry systems with only minor modifications. The proposed method features the ability to augment conventional telemetry data with swimming speed measurements without additional costs in tag size or complexity, promoting richer and more diverse datasets. The technique could potentially become a useful *in-situ* research tool with applications within both general fish behavioural biology and the study of fish performance and welfare in marine farms.

* *Corresponding author*. Nortek AS, Vangkroken 2, NO-7491 Trondheim, Norway.
E-mail address: waseem.hassan@nortekgroup.com (W. Hassan).

https://doi.org/10.1016/j.biosystemseng.2022.05.013

1. Introduction

Aquaculture production has been steadily increasing its respective share of the overall sea-based global food production and it is expected to grow further in future (FAO, 2020). Marine aquaculture using floating fish farms has proven to be a competitive and efficient method for Atlantic salmon production (Iversen et al., 2013) and has resulted in salmon farming becoming one of the most successful sectors within aquaculture. A typical marine fish farm consists of 8–16 floating cages (usually up to 50 m diameter and 40 m depth) that are attached to a common mooring structure that is anchored to the seabed. Each of these cages may hold up to 200,000 fish, thus a modern fish farm may contain millions of individual animals. Traditionally, marine farms have been placed at sheltered locations close to shore to facilitate easy access from land and protect the farm and the farmers from the storms and other demanding conditions. However, the growth in aquaculture and competing claims from other industries has led to a scarcity of new suitable farming locations that has stimulated a trend where fish farming operations are moved to more exposed, even offshore, sites (Bjelland et al., 2015). This trend has also been stimulated by the desire to exploit the lower pathogen and parasite pressures at locations further from shore but may lead to challenges in other areas due to remoteness and increased exposure to undesirable environmental conditions.

Monitoring of farmed animals is essential for good farm management as it is necessary to know the behaviour and welfare status of the animals when planning critical farming operations. In Norway, fish welfare monitoring is required by law for commercial fish farms. However, this can be particularly challenging in aquaculture compared with terrestrial farming due to the practical limitations incurred by working underwater and the sheer biomass and number of animals present in fish farms (Føre et al., 2018), a situation that is further exacerbated at more exposed sites. At present, the most common methods for monitoring and observing fish in commercial fish farms are direct observation either from the surface or through underwater cameras. Recordings can also be post-processed or analysed manually or via an automated machine vision system (Williams et al., 2006). In recent years, approaches using machine vision have resulted in more objective and operational methods for observing fish (Pinkiewicz et al., 2011). Such solutions can be used to quantify various behavioural (e.g., motion (Shinsuke et al., 2011), anomalous activity (Eguiraun et al., 2014)) or exterior (e.g., size (Lines et al., 2001), skin condition (Shinsuke et al., 2011)) properties of fish. Other existing technologies relevant for observing fish in sea-cages include acoustic systems such as echosounders, sonars and split-beam sonars (Klebert et al., 2015; Rundtop & Frank, 2016). Acoustic instruments have been successfully used to monitor different properties in farmed fish populations including swimming speed (Arrhenius et al., 2000), and body length and mass (Soliveres et al., 2017). While both optical and acoustic techniques are not very intrusive, in the sense that they do not need to interact directly with the fish to collect data, they do have some limitations. Factors such as water turbidity, camera movements and recording under low light levels, e.g., during night, can degrade video quality, and the high absorption of light underwater makes camera solutions range limited. Acoustic methods on the other hand, may suffer challenges in separating individual animals when there are several fish within the beam, meaning that their ability to provide data on individuals decreases with fish density. Moreover, both optical and acoustic instruments have limited fields of view and can only provide instantaneous data on the fish or group of fish currently within the observation field. This makes it difficult to obtain insight into individual animal histories, which may be important when assessing cumulative effects of environmental conditions or farming practices on fish performance and welfare.

Acoustic biotelemetry is a commercially available technology that can provide individual based data histories, and as such could complement optical and acoustic methods in providing a more complete picture of the behaviour of fish in marine farms. This method is capable of monitoring individual fish in real-time and has also been tested in commercial marine farms (Rillahan et al., 2009; Føre et al., 2017). A typical acoustic telemetry setup consists of electronic devices called tags and one or more matched acoustic receivers. The tags are either implanted surgically inside the body or attached to the outside of a fish and transmit an encoded acoustic signal containing a unique identifier (ID) and sometimes a data payload from one or more onboard sensors. This signal is received and processed by the acoustic receivers, providing a timestamped decoded ID and data payload to the user (Føre et al., 2011; Pincock & Johnston, 2012). Recent developments within electronics miniaturisation have rapidly extended the range of sensors possible to integrate in acoustic tags, and it is today possible to measure for example temperature (Koeck et al., 2014), depth (by measuring pressure) (Skilbrei et al., 2009), swimming activity (accelerometers) (Broell et al., 2013), ambient light (Cooke et al., 2012), body attitude and orientation (accelerometers) (Føre et al., 2011), oxygen (Svendsen et al., 2006) and electromyography (EMG) (Cooke et al., 2004).

Individual swimming speed data could be a key element in understanding a fish's behavioural dynamics and interaction with the environment, stress, hunger level and for gauging welfare issues related to events such as extreme waves and currents at exposed farming sites (Hvas et al., 2017; Hvas & Oppedal, 2017; Remen et al., 2016). Although average speeds of fish can be measured using consecutive fish positions obtained with algorithms such as time difference of arrival (TDoA) (Rillahan et al., 2009), the accuracy of such estimates will depend on the sampling rate and timing precision of the underlying fish positioning algorithm (Cooke et al., 2004). An alternative approach to obtaining individual histories on swimming speed that is less sensitive to the properties of the telemetry system could be to instantaneously assess swimming speed. Despite that there are solutions able to provide such data for larger aquatic animals (Gabaldon et al., 2019), there exist no acoustic telemetry systems that can measure this for individual free-ranging moderately sized (700 mm) farmed Atlantic salmon directly.

In this study, a novel concept for measuring the instantaneous swimming speed of free-ranging fish was tested in a

full-scale trial to evaluate its feasibility as a tool for observing the behaviour of farmed fish. The method exploits that the acoustic carrier wave of the signal from a tag is subject to a Doppler shift when the tag is moving relative to a receiver. A novel Doppler speed computation algorithm has therefore been developed and verified through laboratory and field experiments reported in Hassan et al. (2020) and Hassan et al. (2019). However, these experiments did not feature measurements from live and freely swimming fish, and hence these studies serve as purely technical proof-of-concept studies. The present study seeks to advance the method a step further by testing the Doppler speed computation algorithm with live fish carrying acoustic tags. This entailed developing a custom-made acoustic tag emitting pulses of sufficient duration to run the Doppler-based speed computation analyses. Five Atlantic salmon (*Salmo salar* L.) were surgically implanted with these customised acoustic tags and were monitored via an array of hydrophones in a large-scale sea cage at a fully stocked marine farm. The raw acoustic signal was acquired from two of the tagged fish over a period of 19 h and Doppler based swimming speed measurements were computed and analysed. In addition to verifying the viability of the method in a realistic situation, the experiment also helped identify how the algorithm and custom tag design can be further developed to improve the method.

2. Materials and methods

2.1. Ethical statement

Fish handling and surgery was done in compliance with the Norwegian Animal Welfare Act (2009), and the experiment was approved by the local responsible animal science laboratory specialist under the surveillance and approval of the Norwegian Animal Research Authority (NARA) (ID 20/23265).

2.2. The speed computation algorithm

When there is relative movement between an acoustic tag and one or several receivers, the frequency of a signal emitted by the tag will undergo a Doppler shift and appear as Doppler shifted frequencies (DSF) at the receivers. The nature of the shift depends on whether the transmitter is moving towards (increased frequency) or away from (decreased frequency) the receiver. When a tag is implanted in a fish, this shift will thus depend on the movement of the fish relative to the receiver. The proposed speed computation algorithm is presented in Hassan et al. (2020), and Fig. 1 schematically illustrates how the method can be applied to measure the speed of a fish in 2D (Fig. 1a) and 3D (Fig. 1b) using multiple receivers.

If the position of the fish O is known and the receivers are stationary, fish speed v_s in 3D can then be calculated by using (Hassan et al., 2020):

$$v_s \frac{f_{dB} c}{f_s \cos\theta_B \sin\xi_s \cos\gamma} \quad (1)$$

where c is the speed of sound in water, f_{dB} is the DSF observed at receiver B, f_s is the frequency of the acoustic signal emitted by the tag, θ_B is the angle between the line *OB* and v_s, γ is the angle between the line *OC* and the depth plane spanned by receivers A, B and C, and ξ_s is the angle between the tag velocity vector and the z-axis (Fig. 1b). The speed of sound in seawater can be calculated by using (Grosso, 1974):

$$c = 1448.6 + 4.618T - 0.0523T^2 + 1.25(S-35) + 0.017D \quad (2)$$

where *T* is the water temperature, *S* is salinity, and *D* is depth. The algorithm first calculates fish speed in 2D using two of the acoustic receivers placed in the *xy*-plane and the 3D fish position as an input. The 3D fish speed is then calculated by measuring ξ_s using the receivers placed in the *yz*-plane (i.e., C and D, Fig. 1b) and eq. (1). The three receivers in the *xy*-plane (i.e., A, B and C, Fig. 1a) are also used for fish positioning based on the TDoA algorithm (Fang, 1990). Finally, the tag velocity vector angle (θ_S) relative to the *x*-axis can be calculated using:

$$\theta_s = 360^\circ - \theta_B - \angle BOX \quad (3)$$

where the $\angle BOX$ (Fig. 1a) is the angle defined by the position of the tag and receivers A and B (Hassan et al., 2020). The detailed steps in the derivation of the proposed Doppler speed computation algorithm are given in Hassan et al. (2020).

Using the setup shown in Fig. 1, it is thus possible to use all four receivers to obtain tag position and find the swimming speed using the Doppler speed computation algorithm by applying frequency analysis (e.g., Fast Fourier Transform, FFT) at three of the acoustic receivers. Placing receivers, A, B and C at the vertices of an equilateral triangle spanning the area of interest, will minimise the positioning errors from the TDoA algorithm, and hence yield a better foundation for accurately assessing swimming speed.

2.3. Design of a Doppler tag

Since the acoustic pulse length directly affects the velocity resolution of the Doppler speed computation algorithm (Hassan et al., 2020; Hovem, 2007; Lhermitte & Serafin, 1984), the tag used in this study had to emit pulses with extended duration. A pulse length of 10 ms, which is commonly used in conventional tags, would yield a speed resolution of 1 ms^{-1}. This is within the expected range of the maximum sustained swimming speed of an adult Atlantic salmon (e.g., 910 mm s^{-1} (Tang & Wardle, 1992)) rendering the standard pulses emitted by commercial tags unsuitable for the Doppler speed computation algorithm. The first studies using the present Doppler method found that a minimum pulse duration of 100 ms is required for the method to result in a reasonable speed resolution (<100 mm s^{-1}) and that increasing the pulse duration will generally improve the resolution (Hassan et al., 2020). A custom-made acoustic tag with an on-board depth sensor was therefore designed to accommodate the requirements of the acoustic pulse signal. The hardware design of the custom tag was identical to an existing and commercially available fish tag (D-LP13, Thelma Biotel AS, Trondheim-Norway), with a cylindrical shape, a diameter of 13 mm and a length of 31 mm, and weighing 5.6 g in water. However, the firmware of the tag was modified to transmit a train of eight consecutive pulses (carrier wave bursts) with 200 ms pulse width and inter-pulse intervals of 300 ms followed by an intermission (silent guard time) of 2.5 s, before transmitting

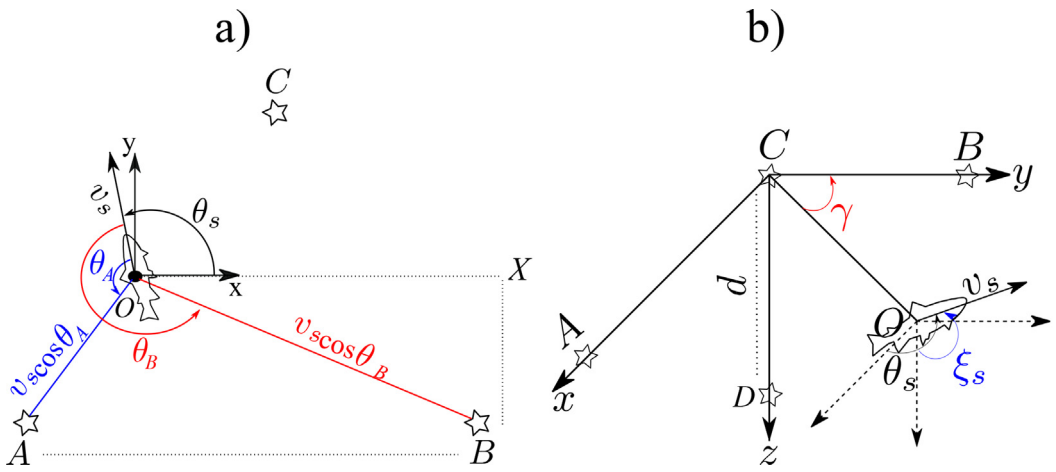

Fig. 1 – a) A tagged fish swimming with a speed v_s making an angle θ_s with the x-axis shown in 2D. Receivers A and B are used by the speed computation algorithm, while all receivers (A, B and C) are used to find fish position through the TDoA algorithm. θ_A and θ_B are the angles between $\rightarrow v_s$ and the lines OA and OB, respectively. b) the same setup as in a) but with a receiver setup to obtain 3D speed. A fourth acoustic receiver D is then placed at depth *d* beneath C and is used together with C to find the angles γ and ξ that are required to determine the 3D speed.

the conventional differential pulse position modulated (DPPM) signal that encodes the unique tag ID and the current depth (pressure) sensor value (Fig. 2). This pulse sequence was repeated every 15 s. Decoding the depth value from the DPPM signal using conventional telemetry receivers thus provided some redundancy in terms of determining the vertical position of the tag, which is crucial for the Doppler algorithm. A total of six acoustic tags were produced for the study. The main rationale behind using several tags was redundancy and experimental robustness in case of fish mortality, tag malfunctioning or other technical challenges during initial testing of the tags. The tags were programmed at six unique frequencies with nominal values of 67 kHz, 68 kHz, 69 kHz, 70 kHz, 71 kHz and 72 kHz. The exact centre frequencies of all tags were measured and profiled for temperature variations in the range 6 °C–15 °C prior to the field experiment. All centre frequencies were also re-calculated based on a benchmark dataset collected at start of the field experiment when all tags were kept stationary at a known position in the sea cage for a period of 20 h.

2.4. *Field experiment*

A field experiment with live fish was carried out in a commercial scale with a fully stocked marine sea-cage containing approximately 172,000 Atlantic salmon.

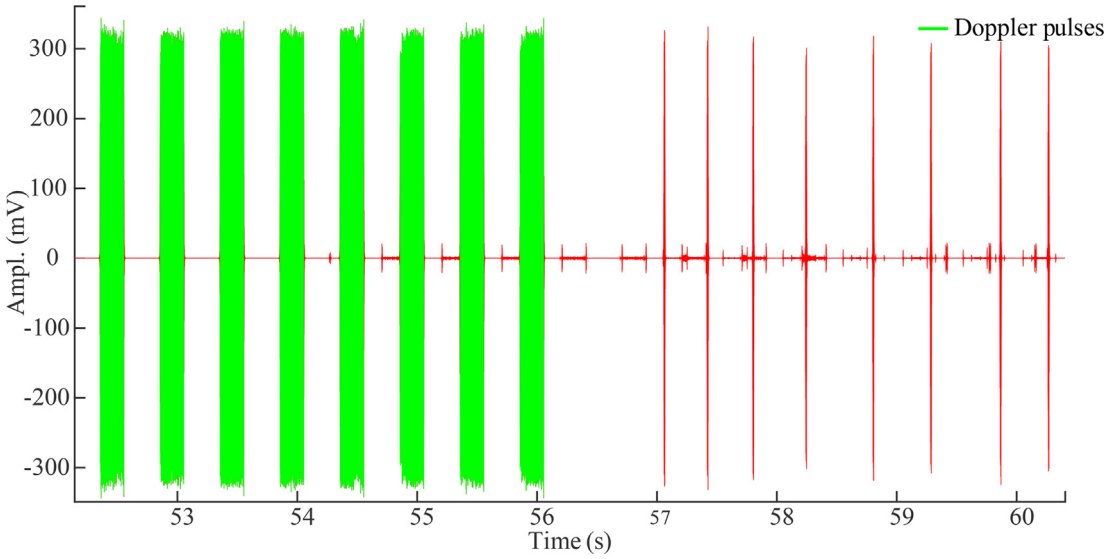

Fig. 2 – Example of the signal received from a single transmission by the custom-made acoustic tag. The signal consists of a burst of eight (200 ms pulses (green) followed by a 2.5 s intermission, and then a conventional eight pulse DPPM encoded signal (pulse width 10 ms, red) carrying the tag ID and depth sensor value. (For interpretation of the references to colour in this figure legend, the reader is referred to the Web version of this article.)

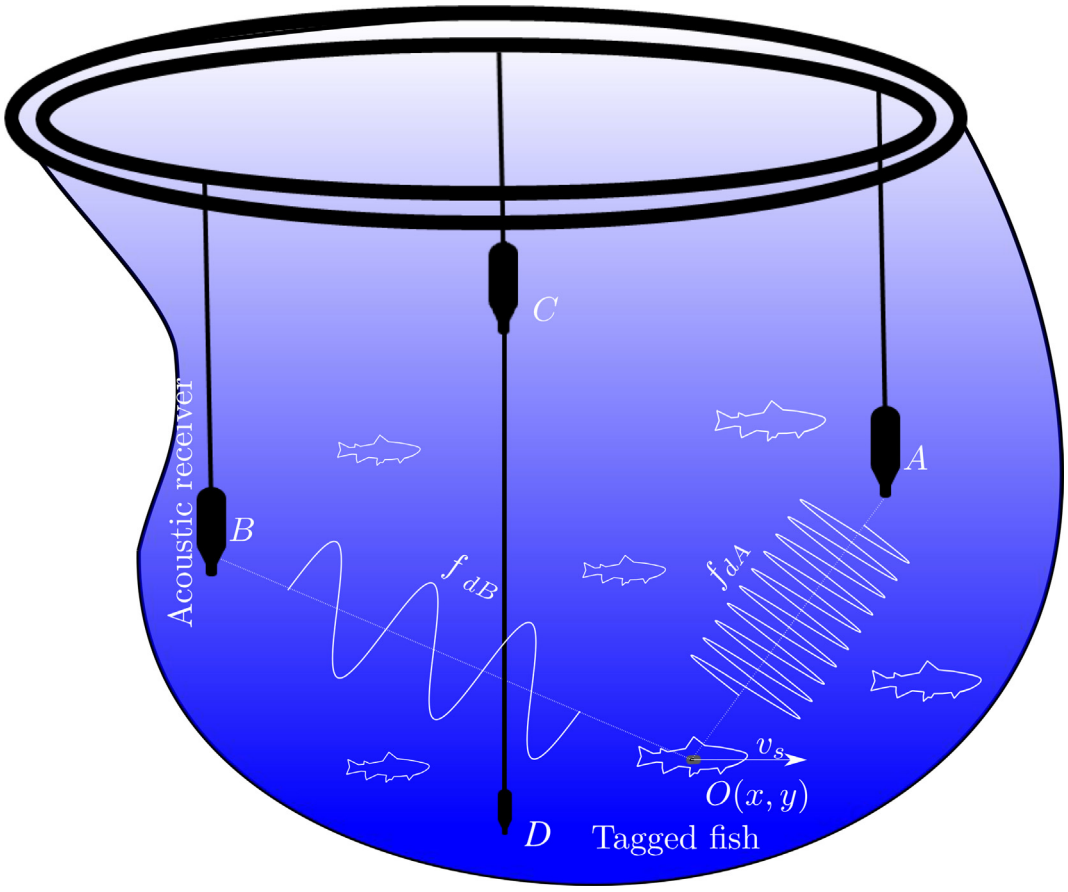

Fig. 3 – Schematic representation of the experimental setup used in the field experiment, showing the tagged fish and the placement of acoustic receivers A, B, C and D. Receivers A, B and C were placed at 2 m depth, forming the *xy* horizontal plane. Receiver D was placed at a depth of 18.5 m and formed the *yz* vertical plane with receiver C.

Figure 3 illustrates the experimental setup. Five fish were randomly caught with a hoop net (ID 110 body length 700 mm, ID 120 body length 620 mm, ID 130 body length 650 mm, ID 140 body length 640 mm and ID 150 body length 720 mm) and tagged intraperitoneally with the Doppler acoustic tags. Surgical procedures for tagging salmon followed a well-documented anaesthesia and surgery protocol (Urke et al., 2013). Fish were anaesthetised using 60 mg l^{-1} tricaine methanesulphonate (MS-222) (Finquel; Argent Chemical Laboratories, Inc., Redmond, WA, USA). After reaching full anaesthesia, the total length of the fish was measured to the nearest millimetre, and the fish was placed in a V-shaped surgical table with a continuous anaesthetic flow over the gills during the entire procedure (40 mg l^{-1} MS-222). A small incision (10–12 mm) was placed slightly offset from the ventral line, about 20 mm behind the pectoral fins. Acoustic tags were sterilised in ethanol, left to air-dry, and inserted through the incision. The incision was closed with three interrupted double surgical knots using non-absorbing 4/0 monofilament suture and sealed with a tissue adhesive (monomeric n-butyl-2-cyanoacrylate, Histoacryl). After the surgical procedure fish were kept in 400 l recovery tanks continuously refreshed with water until reaching full consciousness and were then carefully released into the cage. The sixth Doppler tag (ID 100) was attached to a rope that was tied in at a fixed position on the cage floating collar and submerged with a sinker to 3.4 m depth. During the experiment, this tag served as a nearly static reference exhibiting no other movements than those induced by water current and waves. The reference tag was important in that it enabled establishing the error bounds of the speed measured with the Doppler method.

Three multifrequency acoustic telemetry receivers (TBR-700-RT, Thelma Biotel AS, Trondheim, Norway) were deployed in the sea cage for reception and processing the conventional DPPM signals and logging of the depth sensor values, while four broadband hydrophones (Ocean Sonics Ltd., Nova Scotia, Canada) were used to receive and process the extended pulse length Doppler signals. The clock signals of all receivers and hydrophones were synchronised using the 1-Pulse Per Second (1PPS) signal of the Global Positioning System (GPS) chip inside a custom-made surface module to which they were attached via cables. The three receiver nodes (A, B and C, Fig. 4a) placed in *xy*-plane were used as a primary TDoA-based fish positioning system to provide 2D-positions, while the depth value decoded from the DPPM signal was used to resolve the third dimension. In addition to the surface modules, external batteries (24 V, 32 Ah) were used to extend the operational life of the broadband hydrophones to about ten days.

The hydrophones stored acoustic data in waveform audio format (.wav) using a sampling frequency of 256 kHz and were

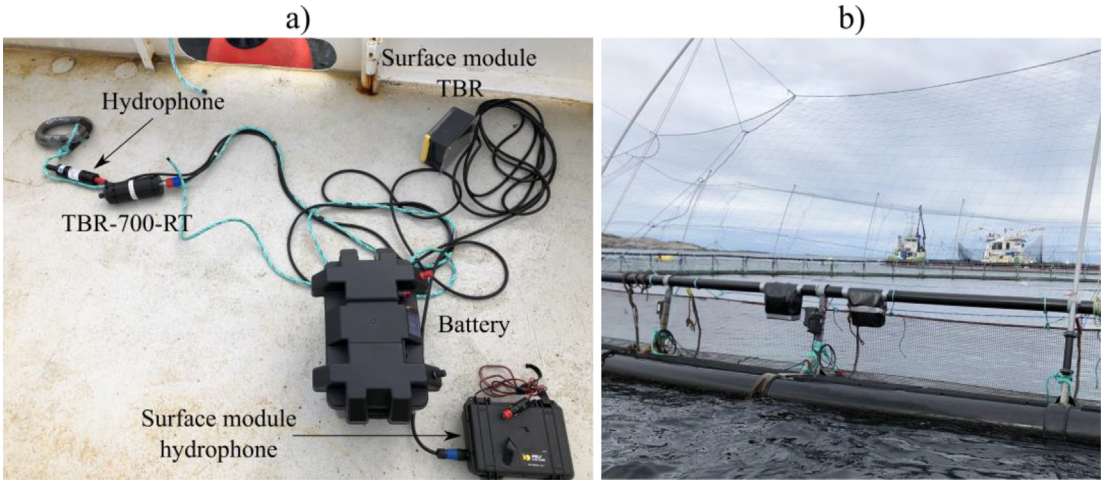

Fig. 4 – a) Single receiver node consisted of a TBR-700-RT acoustic receiver, an Ocean Sonics hydrophone, surface modules for the receiver and hydrophone and a 24 V battery for the hydrophone. b) Receiver nodes C and D mounted onto the cage structure.

configured in a duty cycle logging mode to record three datasets per hour with a duty value of 50% and a period of 1200 s, meaning that the duration of a single dataset was 600 s. The datasets were analysed using Matlab (The MathWorks, Inc., Natick, Massachusetts, USA), employing FFT to find the peak of the frequency spectrum of the received pulse and the corresponding DSF values for the individual pulses in each transmission received from the acoustic tags. The arithmetic mean of all eight DSF values was then used to compute the tag speed. In addition, a matched filter was used to calculate the pulse arrival time for the TDoA positioning algorithm at the three hydrophones (A, B and C) in the horizontal *xy*-plane.

A 20 h duration benchmark dataset was collected at the start of the experiment where all tags were held at a constant depth of 3 m and the hydrophones at a 17% duty cycle (i.e., one 600 s dataset per hour). The tags were then surgically implanted into fish, and the hydrophone duty cycle was changed to 50% (i.e., three 600 s datasets per hour) for the remainder of the experimental period. A conductivity, temperature and depth (CTD) probe was used to profile the water temperature (0–20 m) at the fish farm on day 1, 2 and 3 of the experiment, while temperature was continuously monitored by the TBR-700-RT receivers with an update rate of 600 s. The tagged fish were continuously monitored for twelve days after surgery (i.e., until the tags ran out of power) and appeared to be alive throughout this period.

2.5. *Data management and processing*

In summary, the four hydrophones produced approximately 124 GB data per day, implying that an effective data filtering and management approach was required for their analysis. After basic bandpass filtering to separate the data segments containing the signals from the individual tags based on their centre frequency ($f_s \pm 500$ Hz), all transmissions from each tag were identified. All eight Doppler pulses in each transmission were then subjected to FFT to determine their individual DSF values, before the final speed estimate for the transmission was found by calculating the arithmetic mean of the eight DSF values. Fish positions were found using the TDoA algorithm. Pulse arrival time was calculated by cross correlating the known sent pulse with the received signal at the hydrophones. The depth values for each tag as decoded from the DPPM signals by the TBR-700-RT receivers were synchronised with the arrival time for their respective DPPM signals. In addition, the mean DSF calculation and 2D fish position based on the hydrophone data were synchronised using the arrival time for the Doppler pulses at these. Samples with a speed value of more than 2 ms^{-1} were considered unrealistic in being much higher than expected maximum sustained swimming speeds for Atlantic salmon (Hvas et al., 2017) and marked as outliers without using any advanced filtering techniques.

3. Results

3.1. *Data availability*

Since all six tags were operational at the beginning of the experiment, the plan was to use data from all of them in the ensuing analyses. However, a malfunction in the cable connecting hydrophone D to the surface module led to loss of the 1PPS signal and thus proper synchronisation of this hydrophone. Resolving the 3D-position of the fish is a prerequisite for the Doppler algorithm, and with only three synchronised hydrophones (A, B and C in the horizontal plane) the vertical position of the fish thus had to be obtained from the depth values derived from the DPPM signals by the TBR-700-RT receivers. Since the TBR-units could only monitor three frequencies simultaneously, this meant that depth measurements from only three tags (two fish and the stationary tag) were available, and hence that the other three tags were not used in further analyses.

3.2. Centre frequency calibration

The centre frequencies of all tags were found during the initial on-site benchmarking phase where the tags were held stationary at a fixed position (Table 1). The temperature profiling test showed a maximum variation in centre frequency of 12 Hz with a standard deviation of 6 Hz for all six tags in the range 6 °C–15 °C, however, the average temperatures recorded during the field experiment were almost constant at 14 °C (std. dev. < 0.25 °C) in both time and depth. This implied that the impact of temperature dependent variation was negligible during the trial, hence the centre frequencies obtained from the benchmark dataset could be used directly for calculation of the Doppler shift.

3.3. Speed measurements

Figure 5 shows a histogram of the speeds measured using the Doppler method for three tags over 19 h during the experiment in 200 mm s^{-1} bins. The stationary tag (ID 100, N = 1080) was estimated to have a mean speed of 110 mm s^{-1} (median 80 mm s^{-1}, std. 80 mm s^{-1}) with approximately 90% of the samples laying within the lowest speed interval, i.e., 0 mm s^{-1} to 200 mm s^{-1}. The tags implanted in fish showed a different pattern, both in terms of mean speed and speed distribution. ID 120 (N = 689) had a mean speed of 880 mm s^{-1} (median 750 mm s^{-1}, std. 590 mm s^{-1}) with >50% of the samples in the speed interval 200 mm s^{-1} to 600 mm s^{-1}, whereas ID 140 (N = 699) had a mean speed of 1080 mm s^{-1} (median 1000 mm s^{-1}, std. 560 mm s^{-1}) with 50% of the samples laying in the speed interval 600 mm s^{-1} to 1000 mm s^{-1}.

Figure 6 shows the distribution of the cosine of the angle (θ_s) of $\rightarrow v_s$ for the three tag IDs. The distribution shows a tendency of the tags implanted into fish (IDs 120 and 140) of having a greater variation in θ_s, or less directivity, than the stationary tag (ID 100), for which most of the registrations occurred around 0°. The differences in mean speed were also visible in the time series development for the three tags, with the tags carried by swimming fish being consistently and significantly higher than the reference tag (Fig. 7).

4. Discussion

The stationary reference tag (ID 100) showed consistently lower speed measurements and variability in direction than the tags carried by swimming fish (IDs 120 and 140), demonstrating that the Doppler method was able to distinguish a moving tag from a non-moving tag as well as quantify its speed. This suggests that the method has potential as a tool for remote measurement of the swimming speed of free-ranging individual fish in commercial fish farms as well as in other applications. The low error (i.e., deviation from 0 ms^{-1}) in the mean speed for the stationary tag correspond well with the results from previous experiments using the same method where an error of less than 10% of the total speed range was achieved across all speed ranges (Hassan

Table 1 – Tag IDs and their observed centre frequencies (f_s) during the initial benchmarking phase.

Tag ID	Nominal centre frequency f_{s0} (Hz)	Measured centre frequency f_s (Hz)
100	67,000	66,940
110	68,000	67,989
120	69,000	68,970
130	70,000	69,977
140	71,000	70,982
150	72,000	72,033

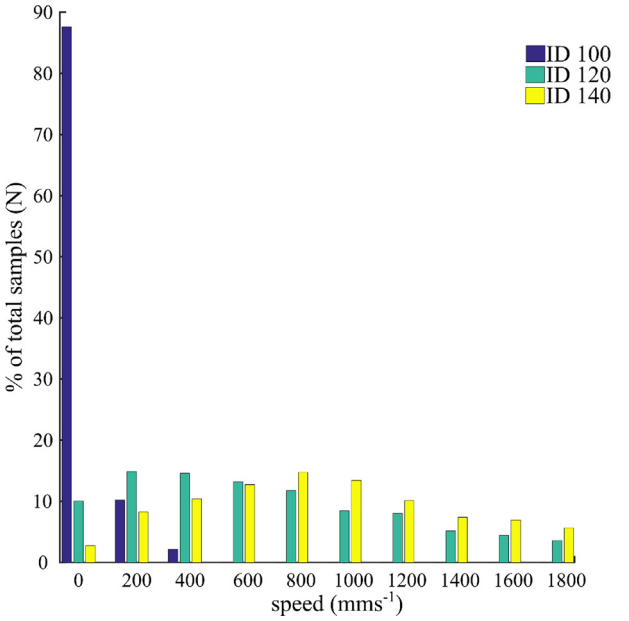

Fig. 5 – Distribution of speed samples estimated for Doppler tag IDs 100 (stationary) and 120/140 (implanted in fish) over a period of 19 h. Bin size 200 mm s^{-1}.

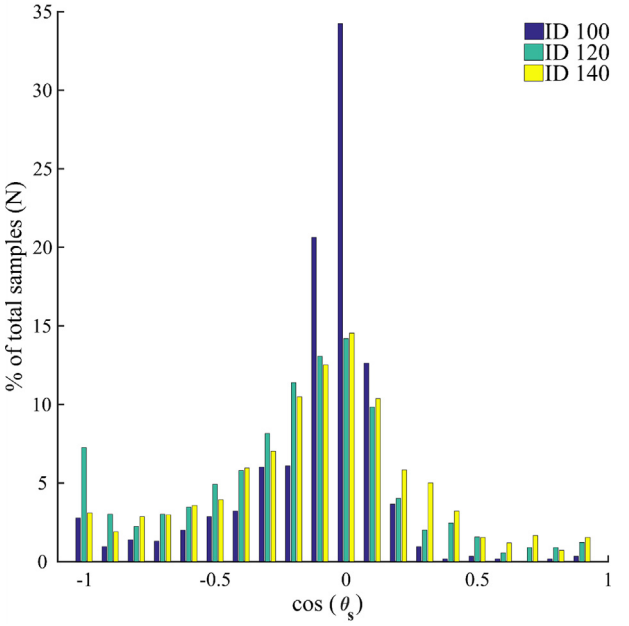

Fig. 6 – Histogram of the measured cos (θ_s) distribution for the three tag IDs. Bin size is 0.1.

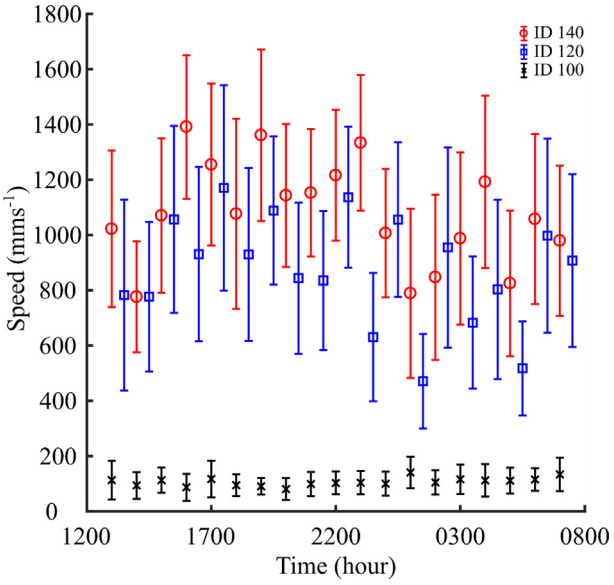

Fig. 7 – Time series of the average speed for three tags recorded over a period of 19 h. Each data point represents hourly averages with standard deviations, and includes three 600 s datasets, each with a number of speed samples in the range 15 < N < 82. All the datasets were collected synchronously, however the dataset for ID 120 has been plotted with an offset of 1800 s for clarity.

et al., 2020), increased the likelihood that the approach is sufficiently sensitive for practical purposes. Furthermore, the mean fish swimming speeds in terms of body lengths per second (1.4 and 1.6 for ID 120 and 140, respectively) seem credible based on the normal range of sustained swimming speed for farmed Atlantic salmon reported in other studies (Hvas et al., 2017; Juell, 1995; Tang & Wardle, 1992), and harmonises with subjective visual observations made at the site during the experiment. Although no ground truth data exist to validate swimming speeds for the tagged fish (which would be difficult to obtain in a practical manner in the large and densely populated sea cage), these similarities suggest that the method was able to assess higher speeds with reasonable accuracy. Moreover, farmed salmon are often observed to adapt circular schooling patterns when kept in sea cages (Oppedal et al., 2011), a pattern that is probably also seen in the measurement data as the distribution of the angle of the velocity vector for the tags carried by the fish was more evenly distributed across all directions than for the stationary tag that was heavily concentrated around 0°. Together, these observations indicate that the tags implanted into the fish were moving with speeds similar to those one might expect for farmed Atlantic salmon, strongly implying that the proposed Doppler speed algorithm offers a new and feasible approach for remote measurement of instantaneous swimming speed in free-ranging fish.

The average speed (and hence error) measured for the stationary tag (ID 100) was slightly higher (110 mm s^{-1}) than the values observed in previous studies using this method (Hassan et al., 2020). This is probably because the Doppler tags developed for this study had a higher standard deviation in centre frequency (6 Hz) than those used in the controlled laboratory and catamaran experiments (<2 Hz, (Hassan et al., 2020)). Although the firmware of the tags used in the present study was tailored to emit pulses of sufficient length to obtain adequate resolution in speed estimates, the hardware was the same as that of the commercially available D-LP13 tag and therefore not optimised with components warranting a very high precision carrier frequency, as was done for the system used in the laboratory studies (Hassan et al., 2020). To compensate for imprecise hardware components, the firmware was set to re-calibrate the internal oscillator of the tag every 500 s. While this compensated for long-term frequency drift and temperature dependency, it also led to sudden shifts in centre frequency that in turn resulted in inaccurate measurements after each re-calibration period. Based on these observations, it is apparent that while the present results show that the Doppler computation algorithm can be used to measure the speed of free-swimming fish, higher accuracy could be achieved by designing a customised acoustic tag with very precise and low tolerance hardware components, and a high precision crystal oscillator.

Despite that the mean error of 110 mm s^{-1} observed for the stationary tag is in accordance with the previous findings using this method, it is also possible that the magnitude of this error could have been influenced by the experimental setup and the prevailing site conditions. While tag 100 was assumed to be stationary, it was held in place using a rope and sinker suspended from the walkway of the cage. This means that the tag would still be affected by water movements (i.e., currents and waves) at the site, which is also the case for the hydrophones. It is therefore possible that part of the mean error seen in the data was caused by that the assumed stationary tag and hydrophones were in fact moving slightly, and thus could be seen as an indirect measurement of random water movements at the site. This notion is supported by the mean error seen in this study agreeing well with the levels of water movement that would be expected at marine farms of this type (Jónsdóttir et al., 2021), a feature also implied by previous average surface currents measured at the site being 40 mm s^{-1}, with current spikes above the average value in some of the measured time series. The fish farm was located at a relatively protected site, close to the shore. A fish farm located at an exposed site away from the shore might experience extreme waves and currents. These adverse weather conditions could lead to a scenario where the assumption that the acoustic receivers are stationary does not hold true all the time. This would result in large errors in the speed measurement. A simple remedy to counter such kind of errors is to use a solid structure such as steel rods for mounting the acoustic receivers. In addition, if the sea-state monitoring instruments are time synchronised with the acoustic receivers, post processing the speed measurement could also help to remove the error induced due to the waves and currents. Finally, the speed measurements could also be corroborated with weather monitoring instruments for their validity at exposed farming sites.

The centre frequencies measured during the on-site benchmarking phase (water temperature 14 °C) proved to be like the values observed in the laboratory. Since the water temperature in the fish cage stayed almost constant, with

variation less than 1 °C both with depth and over time throughout the field experiment, temperature related effects on the centre frequency were therefore not considered as significant.

Although data from only three (IDs 100, 120 and 140) of the six deployed tags were used in the analyses and valid data could only be collected for 19 h, the study yielded sufficient data (i.e., around 700 speed samples for each of ID 120 and ID 140, and 1100 for ID 100) to conclude upon the efficacy of the concept. This was also part of the experimental planning, as tag redundancy was introduced to avoid scenarios such as having malfunctioning tags or post-tagging mortality. The same considerations were made regarding the duration of the experiment, as planning for a longer experimental period increases the likelihood that there will be sufficient periods of valid data for the analyses. It is, however, important to note that if this experiment was designed to investigate behavioural aspects of swimming speed patterns in salmon rather than being a proof-of-concept study, the number of tag replicates in the dataset would have had to be higher and the period would probably have to be longer.

The positioning accuracy of the TDoA algorithm was evaluated by comparing performance when using timestamps from either the TBR-700-RT acoustic receivers or the Ocean Sonics hydrophones. The benchmarking dataset with stationary tags at known positions showed that the hydrophone-based system achieved the highest accuracy with a circular error probability (CEP) value of 2 m, compared to a CEP of 2.75 m for the TBR-700-RTbased system. This can be explained by the TBR-700-RT receiver using a time stamp resolution of 1 ms resulting in a best-case position resolution of 1.5 m in TDoA calculations, while the Ocean Sonics hydrophones have a time stamp resolution of 100 μs giving a best-case position resolution of 0.15 m.

Other approaches for measuring fish swimming speed include swimming tunnel, camera or vision-based solutions and acoustic instruments. A swimming tunnel is straightforward approach for measuring fish swimming capacity (Hvas & Oppedal, 2017; Remen et al., 2016). Fish are forced to swim against a water current with known speed. If the fish is stationary within the tunnel, it maintains a swimming speed equal to the current induced in the tunnel. While being very accurate, the swimming tunnel method could not be used in a marine farm setting and thus does not provide data that is more relevant for a culture setting. One of the popular methods for in-situ measurements is the use of cameras (Pinkiewicz et al., 2011), where a group of fish is recorded, and machine vision algorithms are applied for estimation of swimming speed. Similar observations can also be made using acoustic instruments such as echosounders and split-beam sonars could also be used for fish speed measurement (Pedersen, 2001). However, both video based, and acoustic instruments are limited by the field of view. Video cameras are also limited by turbidity and the propagation characteristics of light in water (Pincock & Johnston, 2012; Williams et al., 2006). In addition, such instruments cannot track individual fish swimming speed over time (Macaulay et al., 2021), as this may allow for more accurate assessments of fish states also on an individual level.

5. Conclusion

The aim of this study was to assess the feasibility of exploiting the Doppler effect and acoustic telemetry to measure instantaneous swimming speeds of individual free-ranging fish. The principle has previously been investigated and deemed feasible using mechanical devices emulating fish movement (Hassan et al., 2020), but proper validation using live fish and genuine acoustic tags was lacking. An experiment was thus conducted in a large-scale fish farm where Atlantic salmon were fitted with biotelemetry acoustic tags augmented with a special Doppler pulse signal. Results from the field experiments demonstrate that the proposed method works well under the conditions encountered in commercial fish farms (sea-cages, 50 m diameter and 40 m depth), and can probably be transferred to other application areas where remote measurement of fish swimming speed is desirable.

Declaration of competing interest

The authors declare that they have no known competing financial interests or personal relationships that could have appeared to influence the work reported in this paper.

Acknowledgement

The authors would like to thank Eirik Svendsen for helping with the application for obtaining the permit for animal experiments, Bjørøya AS for providing an opportunity to conduct the experiment at their fish farm and the NTNU-ITK mechanical workshop for their help on the mechanical setup of the experiment. This work was funded by the Norwegian Research Council through the Centre for research-based innovation in Exposed Aquaculture Technology (grant number 237790) and partly by the "CycLus" R&D project (NTF36/37).

REFERENCES

Arrhenius, F., Benneheij, B. J., Rudstam, L. G., & Boisclair, D. (2000). Can stationary bottom split-beam hydroacoustics be used to measure fish swimming speed in situ? *Fisheries Research*, 45, 31–41. https://doi.org/10.1016/S0165-7836(99)00102-2

Bjelland, H. V., Føre, M., Lader, P., Kristiansen, D., Holmen, I. M., Fredheim, A., Grøtli, E. I., Fathi, D. E., Oppedal, F., Utne, I. B., & Schjølberg, I. (2015). Exposed aquaculture in Norway. In *OCEANS 2015 – MTS/IEEE Washington* (pp. 1–10). https://doi.org/10.23919/OCEANS.2015.7404486

Broell, F., Noda, T., Wright, S., Domenici, P., Steffensen, J. F., Auclair, J.-P., & Taggart, C. T. (2013). Accelerometer tags: Detecting and identifying activities in fish and the effect of sampling frequency. *Journal of Experimental Biology, 216*, 1255–1264. https://doi.org/10.1242/jeb.077396

Cooke, S. J., Hinch, S. G., Lucas, M. C., & Lutcavage, M. (2012). Biotelemetry and biologging. In *Fisheries techniques* (3rd ed., pp. 819–881). American Fisheries Society.

Cooke, S. J., Thorstad, E. B., & Hinch, S. G. (2004). Activity and energetics of free-swimming fish: Insights from electromyogram telemetry. *Fish and Fisheries*, 5, 21–52. https://doi.org/10.1111/j.1467-2960.2004.00136.x

Eguiraun, H., de Ipiña, K. L., & Martinez, I. (2014). Application of entropy and fractal dimension analyses to the pattern recognition of contaminated fish responses in aquaculture. *Entropy*, 16, 6133–6151. https://doi.org/10.3390/e16116133

Fang, B. T. (1990). Simple solutions for hyperbolic and related position fixes. *IEEE Transactions on Aerospace and Electronic Systems*, 26, 748–753.

FAO. (2020). *The state of world fisheries and aquaculture*. Food and Agricultural Organisation of the United Nations.

Føre, M., Alfredsen, J. A., & Gronningsater, A. (2011). Development of two telemetry-based systems for monitoring the feeding behaviour of Atlantic salmon (*Salmo salar* L.) in aquaculture sea-cages. *Computers and Electronics in Agriculture*, 76, 240–251.

Føre, M., Frank, K., Dempster, T., Alfredsen, J., & Høy, E. (2017). Biomonitoring using tagged sentinel fish and acoustic telemetry in commercial salmon aquaculture: A feasibility study. *Aquacultural Engineering*, 78, 163–172. https://doi.org/10.1016/j.aquaeng.2017.07.004

Føre, M., Frank, K., Norton, T., Svendsen, E., Alfredsen, J. A., Dempster, T., Eguiraun, H., Watson, W., Stahl, A., Sunde, L. M., Schellewald, C., Skøien, K. R., Alver, M. O., & Berckmans, D. (2018). Precision fish farming: A new framework to improve production in aquaculture. *Biosystems Engineering*, 173, 176–193. https://doi.org/10.1016/j.biosystemseng.2017.10.014 (Advances in the Engineering of Sensor-based Monitoring and Management Systems for Precision Livestock Farming).

Gabaldon, J., Turner, E. L., Johnson-Roberson, M., Barton, K., Johnson, M., Anderson, E. J., & Shorter, K. A. (2019). Integration, calibration, and experimental verification of a speed sensor for swimming animals. *IEEE Sensors Journal*, 19, 3616–3625. https://doi.org/10.1109/JSEN.2019.2895806

Grosso, V. A. D. (1974). New equation for the speed of sound in natural waters (with comparisons to other equations). *Journal of the Acoustical Society of America*, 56, 1084–1091. https://doi.org/10.1121/1.1903388

Hassan, W., Føre, M., Pedersen, M. O., & Alfredsen, J. A. (2019). A novel Doppler based speed measurement technique for individual free-ranging fish. In *2019 IEEE sensors* (pp. 1–4). https://doi.org/10.1109/SENSORS43011.2019.8956870

Hassan, W., Føre, M., Pedersen, M. O., & Alfredsen, J. A. (2020). A new method for measuring free-ranging fish swimming speed in commercial marine farms using Doppler principle. *IEEE Sensors Journal*, 20, 10220–10227. https://doi.org/10.1109/JSEN.2020.2991294

Hovem, J. M. (2007). Underwater acoustics: Propagation, devices and systems. *Journal of Electroceramics*, 19, 339–347. https://doi.org/10.1007/s10832-0079059-9

Hvas, M., Folkedal, O., Solstorm, D., Vågseth, T., Fosse, J. O., Gansel, L. C., & Oppedal, F. (2017). Assessing swimming capacity and schooling behaviour in farmed Atlantic salmon Salmo salar with experimental push-cages. *Aquaculture*, 473, 423–429. https://doi.org/10.1016/j.aquaculture.2017.03.013

Hvas, M., & Oppedal, F. (2017). Sustained swimming capacity of Atlantic salmon. *Aquaculture Environment Interactions*, 9, 361–369. https://doi.org/10.3354/aei00239

Iversen, A., Andreassen, O., Hermansen, Ø., Larsen, T. A., & Terjesen, B. F. (2013). Oppdrettsteknologi og konkurranseposisjon. In *Rapport 32/2013 Nofima*.

Jónsdóttir, K. E., Volent, Z., & Alfredsen, J. A. (2021). Current flow and dissolved oxygen in a full-scale stocked fish-cage with and without lice shielding skirts. *Applied Ocean Research*, 108, 102509. https://doi.org/10.1016/j.apor.2020.102509

Juell, J.-E. (1995). The behaviour of Atlantic salmon in relation to efficient cage-rearing. *Reviews in Fish Biology and Fisheries*, 5, 320–335. https://doi.org/10.1007/BF00043005

Klebert, P., Patursson, Ø., Endresen, P. C., Rundtop, P., Birkevold, J., & Rasmussen, H. W. (2015). Three-dimensional deformation of a large circular flexible sea cage in high currents: Field experiment and modeling. *Ocean Engineering*, 104, 511–520. https://doi.org/10.1016/j.oceaneng.2015.04.045

Koeck, B., Pastor, J., Saragoni, G., Dalias, N., Payrot, J., & Lenfant, P. (2014). Diel and seasonal movement pattern of the dusky grouper Epinephelus marginatus inside a marine reserve. *Marine Environmental Research*, 94, 38–47. https://doi.org/10.1016/j.marenvres.2013.12.002

Lhermitte, R., & Serafin, R. (1984). Pulse-to-pulse coherent Doppler sonar signal processing techniques. *Journal of Atmospheric and Oceanic Technology*, 1, 293–308. https://doi.org/10.1175/15200426(1984)001<0293:PTPCDS>2.0.CO;2

Lines, J., Tillett, R., Ross, L., Chan, D., Hockaday, S., & McFarlane, N. (2001). An automatic image-based system for estimating the mass of freeswimming fish. *Computers and Electronics in Agriculture*, 31, 151–168. https://doi.org/10.1016/S0168-1699(00)00181-2

Macaulay, G., Warren-Myers, F., Barrett, L. T., Oppedal, F., Føre, M., & Dempster, T. (2021). Tag use to monitor fish behaviour in aquaculture: A review of benefits, problems and solutions. *Reviews in Aquaculture*, 13, 1565–1582. https://doi.org/10.1111/raq.12534

Oppedal, F., Dempster, T., & Stien, L. H. (2011). Environmental drivers of atlantic salmon behaviour in sea-cages: A review. *Aquaculture*, 311, 1–18. https://doi.org/10.1016/j.aquaculture.2010.11.020

Pedersen, J. (2001). Hydroacoustic measurement of swimming speed of North Sea saithe in the field. *Journal of Fish Biology*, 58, 1073–1085. https://doi.org/10.1111/j.1095-8649.2001.tb00556.x

Pincock, D. G., & Johnston, S. V. (2012). Acoustic telemetry overview. In *Telemetry techniques: A user guide for fisheries research* (pp. 305–308). Bethseda, Maryland: American Fisheries Society.

Pinkiewicz, T., Purser, G., & Williams, R. (2011). A computer vision system to analyse the swimming behaviour of farmed fish in commercial aquaculture facilities: A case study using cage-held Atlantic salmon. *Aquacultural Engineering*, 45, 20–27. https://doi.org/10.1016/j.aquaeng.2011.05.002

Remen, M., Solstorm, F., Bui, S., Pascal, K., Vågseth, T., Solstorm, D., Hvas, M., & Oppedal, F. (2016). Critical swimming speed in groups of Atlantic salmon Salmo salar. *Aquaculture Environment Interactions*, 8, 659–664. https://doi.org/10.3354/aei00207

Rillahan, C., Chambers, M., Howell, W. H., & Watson, W. H. (2009). A selfcontained system for observing and quantifying the behavior of Atlantic cod, *Gadus morhua*, in an offshore aquaculture cage. *Aquaculture*, 293, 49–56. https://doi.org/10.1016/j.aquaculture.2009.04.003

Rundtop, P., & Frank, K. (2016). Experimental evaluation of hydroacoustic instruments for ROV navigation along aquaculture net pens. *Aquacultural Engineering*, 74, 143–156. https://doi.org/10.1016/j.aquaeng.2016.08.002

Shinsuke, T., Minoru, K., Kazuyoshi, K., Katsuya, S., & Tsutomu, T. (2011). A digital stereo-video camera system for three-dimensional monitoring of free-swimming pacific bluefin tuna, thunnus orientalis, cultured in a net cage. *Aquatic Living Resources*, 24, 107–112. https://doi.org/10.1051/alr/2011133

Skilbrei, O. T., Holst, J. C., Asplin, L., & Holm, M. (2009). Vertical movements of "escaped" farmed Atlantic salmon (*Salmo salar* L.)—A simulation study in a western Norwegian fjord. *ICES Journal of Marine Science*, 66, 278–288. https://doi.org/10.1093/icesjms/fsn213

Soliveres, E., Poveda, P., Estruch, V., Pérez-Arjona, I., Puig, V., Ordóñez, P., Ramis, J., & Espinosa, V. (2017). Monitoring fish weight using pulse-echo waveform metrics. *Aquacultural Engineering, 77*, 125–131. https://doi.org/10.1016/j.aquaeng.2017.04.002

Svendsen, J. C., Aarestrup, K., Steffensen, J. F., & Herskin, J. (2006). A novel acoustic dissolved oxygen transmitter for fish telemetry. *Marine Technology Society Journal, 40*, 103–108. https://doi.org/10.4031/002533206787353655

Tang, J., & Wardle, C. S. (1992). Power output of two sizes of Atlantic Salmon (*Salmo salar*) at their maximum sustained swimming speeds. *Journal of Experimental Biology, 166*, 33–46. https://doi.org/10.1242/jeb.166.1.33

Urke, H. A., Kristensen, T., Arnekleiv, J. V., Haugen, T. O., Kjærstad, G., Stefansson, S. O., Ebbesson, L. O. E., & Nilsen, T. O. (2013). Seawater tolerance and post-smolt migration of wild Atlantic salmon *Salmo salar* × brown trout *S. trutta* hybrid smolts. *Journal of Fish Biology, 82*, 206–227.

Williams, R., Lambert, T., Kelsall, A., & Pauly, T. (2006). Detecting marine animals in underwater video: Let's start with salmon. In *AMCIS 2006 proceedings 191*.